J Biomol NMR (2007) 37:147–157
DOI 10.1007/s10858-006-9125-7

ARTICLE

^{15}N–{^{1}H} NOE experiment at high magnetic field strengths

Qingguo Gong · Rieko Ishima

Received: 21 August 2006 / Accepted: 20 November 2006 / Published online: 16 January 2007

Abstract The heteronuclear ^{15}N–{^{1}H} NOE values are typically determined by taking the ratio of ^{15}N signal intensities recorded in the presence and absence of ^{1}H saturation prior to evolution of ^{15}N magnetization. Since the intensity ratio of two independent experiments is taken, complete recovery of ^{15}N magnetization during the scan repetition delay is critical to obtain reliable NOE values. Because it may not be practical to wait for the complete recovery of magnetization at high magnetic fields, Solomon equations may be used to correct measured NOE values. Here, based on experiments and simulations, we show that since the cross-correlation between ^{1}H–^{15}N dipole and ^{15}N chemical shift anisotropy becomes significant at high fields for small or deuterated proteins, measured NOE values can not be accurately corrected based on the Solomon equations. We also discuss ranges of rotational correlation times and proton spin-flip rate, in which the NOE values can be corrected by the equations.

Keywords Cross-relaxation · Cross-correlation · Protein · Dynamics · Relaxation · NMR

Introduction

NMR is often used to characterize internal motions of proteins (Dayie et al. 1996; Ishima and Torchia 2000; Fushman and Cowburn 2001; Palmer 2001; Bruschweiler 2003; Redfield 2004; Kay 2005; Jarymowycz and Stone 2006; Igumenova et al. 2006). The ^{15}N–{H} steady-state NOE in proteins is sensitive to motions at frequencies of $\omega_H \pm \omega_N$. In the model-free analysis that widely applied to proteins, the longitudinal (T_1) and transverse relaxation times (T_2) are used together with ^{15}N–{H} NOE values to derive model-free parameters (Palmer 1997). However, the rotational correlation time is a two-valued function of T_1, and T_2 reflects chemical exchange as well as motion at $\omega_H \pm \omega_N$ frequencies. Thus, ^{15}N–{H} NOE is an indispensable component in the model-free analysis to characterize sub-nanosecond motion of proteins (Palmer 1997). One disadvantage of the NOE experiment has been that because the starting magnetization of the ^{15}N–{H} steady-state NOE experiment is ^{15}N, sensitivity of the NOE experiment is ca. 10 times lower than the typical HSQC-based T_1 and T_2 measurements. However, use of recent low-temperature probes significantly increases the sensitivity of the ^{15}N–{H} NOE experiment, and enables accurate quantitative evaluation of ^{15}N–{H} NOE values.

The ^{15}N–{H} steady-state NOE values are determined by taking the ratio of the ^{15}N signal intensities recorded in the presence and absence of proton saturation prior to excitation of ^{15}N magnetization (Kay et al. 1989). There are at least three critical factors that require attention in order to measure reliable NOE values. First, water–amide proton exchange can affect NOE values if the water-flip pulse is not applied (Grzesiek and Bax 1993; Li and Montelione 1994; Skelton et al. 1993). Second, ^{1}H saturation is also important to obtain quantitatively reliable NOE values (Kay et al. 1989; Renner et al. 2002). Third, complete

Q. Gong · R. Ishima (✉)
Department of Structural Biology, School of Medicine, University of Pittsburgh, Rm 1037, Biomedical Science Tower 3, 3501 5th Avenue, 15260 Pittsburgh, PA, USA
e-mail: ishima@pitt.edu

magnetization recovery during the pulse repetition delay is critical for accurate measurement of NOE values. Because ^{1}H and ^{15}N T_1 values become longer as magnetic field strength increases, it may not be practical to wait for a complete recovery of proton magnetization in the NOE experiments at 800 MHz and 900 MHz NMR instruments. Holak's group has quantitatively demonstrated the effects of insufficient pulse repetition time (Renner et al. 2002). In theory, the effect of the insufficient recovery time can be corrected using Solomon equations (Solomon 1955). Correction equations in which cross-relaxation between amide ^{1}H and ^{15}N and extra relaxation sink from surrounding protons have been previously proposed (Freedberg et al. 2002; Grzesiek and Bax 1993; Skelton et al. 1993). In recent publications by other groups (Grzesiek and Bax 1993; Skelton et al. 1993), insufficient recovery of ^{1}H magnetization was taken into account in a correction equation by using experimentally determined ^{1}H T_1 values, whereas in a previous paper (Freedberg et al. 2002) we had accounted for the recovery of both ^{1}H and ^{15}N T_1 values to derive a correction equation.

None of these above-mentioned efforts, however, have explicitly taken the effect of cross-correlation between ^{1}H–^{15}N dipolar coupling and ^{15}N chemical shift anisotropy (DD-CSA) into account (Werbelow and Grant 1977). In the previous derivations, the cross-correlation effect is assumed to be negligible or completely averaged out by fast proton-spin flip rate. The effects of the DD-CSA on ^{15}N T_1 and ^{15}N T_2 have been well studied previously, and been suppressed using pulse sequences that apply ^{1}H 180° pulses, or ^{1}H saturation pulses during the relaxation period (Boyd et al. 1990; Kay et al. 1992; Palmer et al. 1992). In spite of the studies done on the effect of DD-CSA cross-correlation on T_1 and T_2 values, the influence of DD-CSA cross-correlation on the ^{15}N–{^{1}H} NOE experiment has not yet been described.

In this study, we will first show that NOE values determined by the experiments with insufficient scan repetition delay cannot be explained by simple Solomon equations (Solomon 1955) when the apparent amide ^{1}H T_1 values of the sites are long. Therefore, such NOE values cannot be properly corrected by using published equations. We will next show that ^{15}N magnetization recovery in the presence of ^{1}H saturation is expressed by a theoretical curve derived from the Solomon equations, whereas the magnetization recovery in the absence of ^{1}H saturation does not for the sites that have long amide ^{1}H T_1 values. The magnetization recovery in the absence of ^{1}H saturation for these sites can be explained using Goldman's equations which take into account cross-correlation between ^{15}N (or ^{1}H) chemical shift anisotropy and ^{1}H–^{15}N dipolar interaction (Goldman 1984). Finally, we will describe rotational correlation times and proton spin-flip rates for which the cross-correlation effect is significant, and discuss a strategy to determine ^{15}N–{H} NOE values at high magnetic fields.

Methods

Theory

Time dependence of longitudinal relaxation of a ^{1}H–^{15}N two-spin system is typically expressed using the Solomon equations (Solomon 1955). From the solution of the Solomon equation (for example, Eq. [5.17] in the reference Cavanagh et al. 1996), ^{15}N longitudinal magnetizations that recover in the absence and presence of ^{1}H saturation, $\mathrm{N_Z^{nonsat}}(t)$ and $\mathrm{N_Z^{sat}}(t)$, respectively, are expressed by the following equations.

$$\mathrm{N_Z^{nonsat}}(t) = \mathrm{N_Z^0}(1 - \mathrm{e}^{-t/T_{1N}}) - \frac{\sigma_{HN}\mathrm{H_Z^0}(\mathrm{e}^{-t/T_{1N}} - \mathrm{e}^{-t/T_{1H}})}{(1/T_{1N} - 1/T_{1H})} \quad (1)$$

$$\mathrm{N_Z^{sat}}(t) = \mathrm{N_Z^0}(1 - \mathrm{e}^{-t/T_{1N}}) + T_{1N}\sigma_{HN}H_Z^0(1 - \mathrm{e}^{-t/T_{1N}}) \quad (2)$$

Here, ^{15}N T_1 and ^{1}H T_1 are noted as T_{1N} and T_{1H}, respectively. σ_{HN} is a cross-relaxation term between ^{15}N–^{1}H dipolar interaction. N_Z^0 and H_Z^0 are Zeeman equilibrium magnetizations of ^{15}N and ^{1}H spins, respectively. From Eqs. (1) and (2), it is obvious at $t \rightarrow \infty$, $N_Z^{nonsat}(t)$ approaches N_Z^0 and $N_Z^{sat}(t)$ approaches $N_Z^0(1 + T_{1N}\sigma_{HN}H_Z^0)$. Therefore, the NOE enhancement value determined by the ratio of $\mathrm{N_Z^{sat}}(t)$ and $\mathrm{N_Z^{non}}(t)$ is

$$\mathrm{NOE} = \frac{\mathrm{N_Z^{sat}}(t)}{\mathrm{N_Z^{nonsat}}(t)} = \mathrm{N_Z^0} + T_{1N}\sigma_{HN}\mathrm{H_Z^0} = 1 + \frac{\gamma_H}{\gamma_N}T_{1N}\sigma_{HN} \quad (3)$$

As described previously (Freedberg et al. 2002; Grzesiek and Bax 1993; Skelton et al. 1993), Eqs. (1–3) can be used to derive the following simple relationship.

$$\mathrm{NOE_m} = \frac{\mathrm{NOE}}{1 - f(1 - \mathrm{NOE})} \quad (4)$$

Here, $\mathrm{NOE_m}$ and NOE indicate the measured and the theoretical NOE values, and the $\mathrm{NOE_m}$ is given by $\mathrm{N_Z^{sat}}(t)/\mathrm{N_Z^{non}}(t)$. f is defined by (Freedberg et al. 2002)

$$f = \left(\frac{T_{1H}}{T_{1H} - T_{1N}}\right)\left(\frac{e^{-t/T_{1H}} - e^{-t/T_{1N}}}{1 - e^{-t/T_{1N}}}\right) \quad (5)$$

When T_{1N} is sufficiently small (or t is sufficiently large) to satisfy the condition of $\exp(-t/T_{1N}) \approx 0$, f simplifies to $f = \exp(-t/T_H)$ as described previously (Grzesiek and Bax 1993; Skelton et al. 1993).

Simulation of ^{15}N magnetization recovery

In the above theory, the effect of spin diffusion is taken into account in the manner that the T_{1H} is an effective relaxation time that includes the effect of spin diffusion from surrounding protons to the amide proton, but cross-correlation between ^{15}N (or ^{1}H) chemical shift anisotropy (CSA) and ^{1}H–^{15}N dipolar interaction is not accounted for. Both effects are taken into account using the theory of Goldman (Goldman 1984), which shows that:

$$\frac{d}{dt}\begin{bmatrix} N_Z \\ H_Z \\ 2N_ZH_Z \end{bmatrix} = -\begin{bmatrix} 1/T_{1N} & \sigma_{NH} & \eta_N \\ \sigma_{NH} & 1/T_{1H}+1/T_{HH} & \eta_H \\ \eta_N & \eta_H & 1/T_{N_ZH_Z} \end{bmatrix} \times \begin{bmatrix} N_Z - N_{Z,eq} \\ H_Z - H_{Z,eq} \\ 2N_ZH_Z \end{bmatrix} \quad (6)$$

Here, η_N is the relaxation rate due to cross-correlation between the ^{1}H–^{15}N dipole and ^{15}N CSA, and η_H is the relaxation rate due to cross-correlation between the ^{1}H–^{15}N dipole and ^{1}H CSA. The equilibrium magnetization of ^{1}H and ^{15}N are indicated by $N_{Z,eq}$ and $H_{Z,eq}$, respectively.

We numerically calculated the time-dependence of the recovery of the ^{15}N magnetizations, $N^{(1)} = N_Z + N_ZH_Z$ and $N^{(2)} = N_Z - N_ZH_Z$, using Eq. (6) under the following three conditions. (I) First, we simulated Freeman–Hill type (Freeman and Hill 1971; Sklenar et al. 1987) decay of the two components ($N^{(1)}$ and $N^{(2)}$) at a variable time assuming 500 MHz and 800 MHz operating proton frequencies. In the Freeman–Hill approach, the decay of the difference between two scans is taken in which N_Z has respective values of $N_Z(0)$ and $-N_Z(0)$. This simplifies the solution of Eq. (6) to $u(t) = \exp(-Mt) \cdot u(0)$. Here, $u(t) = [N_Z^0, H_Z^0, 2N_ZH_Z^0]$, and M is the 3×3 relaxation matrix in Eq. (6). Therefore, in this simulation, the initial condition is $[N_Z^0, H_Z^0, 2N_ZH_Z^0] = [1, 0, 0]$, and magnetizations relax to [0, 0, 0], as in recent T_1 relaxation experiments based on the original work by Sklenar et al. (1987). (II) Second, we calculated a recovery of the sum of the $N^{(1)}$ and $N^{(2)}$ magnetization as a function of time, starting with the initial condition of $[N_Z^0, H_Z^0, 2N_ZH_Z^0] = [0, 0, 0]$ and reaching to an equilibrium of [1, 1, 0]. This mimics the experimental condition of the $N_Z^{nonsat}(t)$ recovery experiments described below. (III) Third, we calculated the decay of $N^{(1)}$ and $N^{(2)}$ as a function of the effective rotational correlation time, at a decay time of 3 s. We started with the initial condition of $[N_Z^0, H_Z^0, 2N_ZH_Z^0] = [1, 0, 0]$ in order to assess how the rotational correlation time affects the cross-correlation effect. In the simulation, relaxation matrix elements were calculated assuming a single rotational correlation time. CSA values for ^{15}N and ^{1}H were assumed to be 170 and 17 ppm, respectively. In simulations (1) and (2), we also included the effect of external protons by adding an additional amide ^{1}H relaxation rate of 0.5 s^{-1} to account for ^{1}H–^{1}H dipolar interactions of 0.5 s^{-1}, and by an additional $2H_ZN_Z$ relaxation rate due to ^{1}H spin flip effects (Kay et al. 1992) of either 1.5 s^{-1} or 1,000 s^{-1}. In simulation (3), we included a ^{1}H–^{1}H dipolar interaction assuming one ^{1}H–^{1}H dipolar interaction with an internuclear distance, r_H, of either 2.7 Å or 1.9 Å, to provide the effect of the external protons.

Experiments

All NMR relaxation experiments were performed using 0.8 mM deuterated ^{15}N-labeled ubiquitin (Spectra Isotope) in a 20 mM acetate buffer at pH 5.0. NMR spectra at 17°C were recorded on a Bruker DRX800 spectrometer operating at a ^{1}H frequency of 800.13 MHz and using a triple-resonance cold-temperature probe with a shielded z-gradient coil, unless otherwise noted. Under these conditions, the water–amide exchange is expected to be slower than 1 min. Therefore, we did not take into account the effects of water–amide proton exchange.

^{15}N magnetization recovery in the presence and absence of ^{1}H saturation was recorded using a typical pulse sequence for ^{15}N–{^{1}H} NOE experiment with the following minor modifications (Grzesiek and Bax 1993). (1) After a 7 s scan repetition delay, ^{15}N and ^{1}H 90° pulses are applied followed by a gradient. (2) A variable delay was applied with/without ^{1}H saturation. (3) An ^{15}N 90° pulse is applied to record ^{15}N magnetization for t_1 evolution followed by the INEPT transfer for ^{1}H detection (Fig. 1). Since we modified only the initial portion of the pulse sequence and acquisition order of the typical ^{15}N–{^{1}H} experiment, we show only a simple flow diagram of the pulse sequence in Fig. 1. The ^{1}H saturation was achieved by applying 120° ^{1}H pulses with 10 ms delay (Kay et al. 1992), and applied for durations of 0.1, 0.2, 0.4, 0.5, 0.6, 0.8, 1.0, 3.0, and

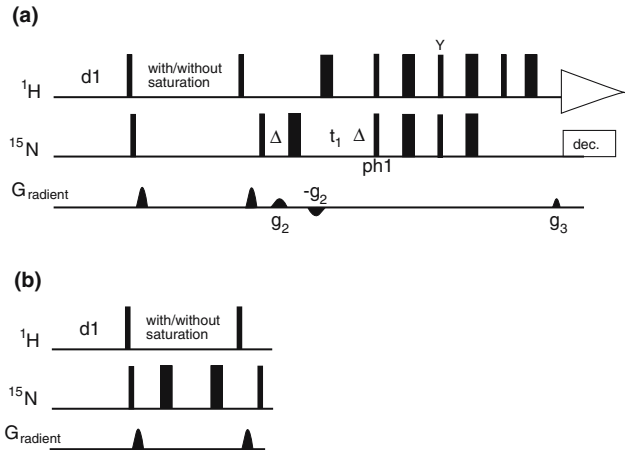

Fig. 1 (**a**) Simple pulse schemes for the modified NOE experiments to detect magnetization recovery in the presence and absence of ^{1}H saturation, and (**b**) a portion of the magnetization recovery to suppress the cross-correlation effect. After the initial delay (d1), the transverse ^{15}N and ^{1}H magnetization is dephased. The delay followed by the d1 period was varied as described in the experimental section. Two series of experiments were performed, one in the presence and one in the absence of ^{1}H saturation during this variable delay time. The ^{1}H saturation was achieved by applying 120° ^{1}H pulses in every 10 ms (Kay et al. 1989; Renner et al. 2002). Original phase cycles and gradients as described in the Bruker pulse sequence library (Bruker, Billerica, USA) were applied after the second ^{15}N pulse

4.0 s. The delays without ^{1}H saturation were 0.1, 0.3, 0.5, 0.7, 1.0, 2.0, 3.0, 4.0, and 6.0 s. Using the data acquired in the presence and absence of ^{1}H saturation, NOE values were calculated as a function of the delay time.

In the above experiments, the initial condition of the magnetization recovery is set to $N_Z(0) = H_Z(0) = 0$. This is because at the end of acquisition, ^{1}H magnetization decays quickly by T_2, and ^{1}H Z-magnetization recovery starts from 0. Similarly, ^{15}N magnetization that is decoupled during the acquisition period is 0 at the end of the acquisition period. Therefore, the 7 s scan repetition delay is not for recovery of Z-magnetization because the magnetization recovery starts after the 90° pulse and the gradient. Rather, we added the long delay to eliminate possible contribution of two-spin order terms that remain after the acquisition period prior to the start of the next experiment. Ideally, even if $2H_ZN_Z$ term remains, it is converted to multi/zero-quantum coherence by the 90° pulses and should decay during the magnetization recovery delay.

Non-selective inversion recovery experiments were performed to determine ^{1}H T_1 and ^{15}N T_1 values, respectively, using typical pulse sequences based on the ^{1}H–^{15}N HSQC and the ^{1}H–^{15}N refocused HSQC (Freedberg et al. 2002). Spectra for ^{1}H T_1 relaxation were recorded with relaxation delay times of 0.0, 0.5, 1.0, 2.0, 3.0, and 4.0 s. Since the ^{1}H T_1 values are used to estimate the rate of recovery of magnetization for NOE experiments, the relaxation period was placed to precede the start of the HSQC sequence to establish a non-selective inversion recovery. The scan repetition delay for the ^{1}H T_1 experiment was set to be 7.5 s, which is less than three times the typical T_1 value of our sample. However, the short delay does not affect the T_1 measurement because the Freeman–Hill method (Freeman and Hill 1971; Sklenar et al. 1987) is applied in a manner similar to the typical T_1 experiments. In the ^{15}N T_1 experiment, spectra were recorded with relaxation delays of 0.1, 0.2, 0.3, 0.5, 0.7, and 0.9 s. The acquisition of ^{1}H T_1 and ^{15}N T_1 spectra took 20 and 12 h, respectively.

The $2H_ZN_Z$ relaxation was measured with the relaxation delays of 0.0, 0.02, 0.04, 0.08, 0.16, 0.24, 0.32, 0.4, and 0.48 s, using the pulse scheme published previously (Boyd et al. 1990; Kay et al. 1992; Muhandiram et al. 1995). Using the $2H_ZN_Z$ relaxation time and ^{15}N T_1, the proton-spin flip time, T_{sf}, was determined using Eq. (7).

$$1/T_{sf} = 1/T_{2N_ZH_Z} - 1/T_{1N} \tag{7}$$

All data were processed using nmrPipe and nmrDraw software (Delaglio et al. 1995; Garrett et al. 1995). Relaxation times were determined by fitting a single-exponential function to the decay of signal intensities using non-linear least square minimization. Uncertainties of the relaxation times were estimated by the Monte-Carlo method. Uncertainty in the NOE value was estimated based on signal-to-noise ratios of the peak intensities.

Results

Magnetization recovery curves that exhibit $NOE_m > 1.0$

Using the modified pulse scheme for the ^{15}N–{^{1}H} NOE experiment (Fig. 1), ^{15}N magnetization recovery was recorded in the presence and absence of ^{1}H saturation. As shown in Fig. 2, the excited magnetization recovers from 0 to 1 or to a saturated intensity in the absence or presence of ^{1}H saturation, respectively. The typical signal-to-noise ratio of the peaks at 6 s when using ^{1}H saturation was 150–300. Therefore, even for this highly sensitive ubiquitin sample, use of a cold-temperature high-sensitivity probe was indispensable to acquire the series of 2D spectra of the ^{15}N–{^{1}H}

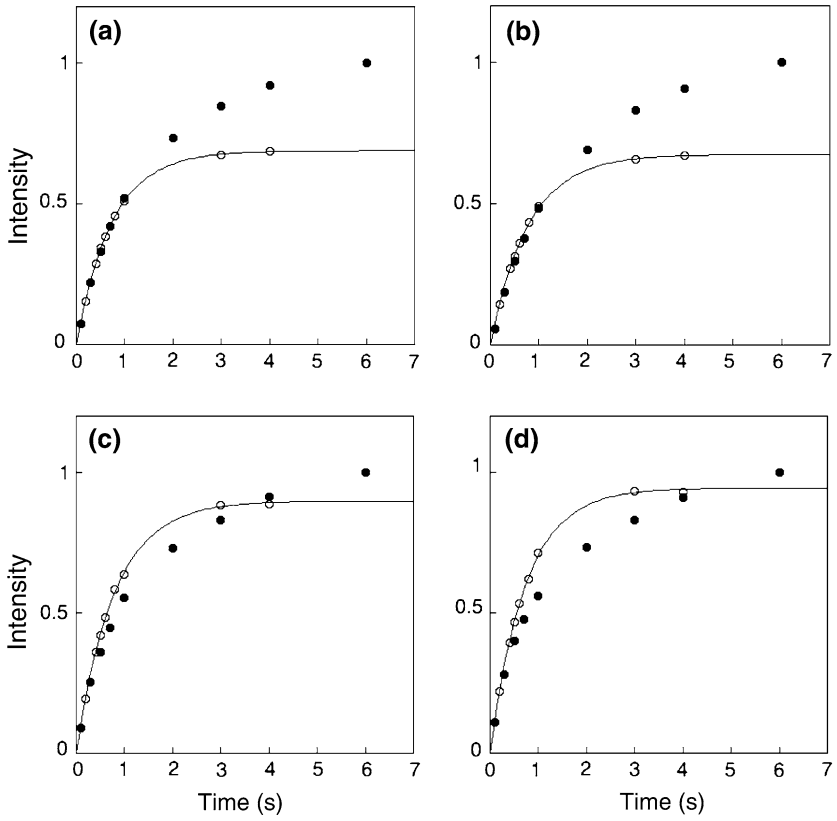

Fig. 2 Recovery of ^{15}N magnetizations for (**a**) residue 8, (**b**) residue 9, (**c**) residue 5, and (**d**) residue 6. Intensities of the magnetizations, $N_Z^{sat}(t)$ (*open circle*) and $N_Z^{nonsat}(t)$ (*closed circle*), were recorded in the presence and absence of proton saturation, respectively. Residue numbers were tentatively assigned from the similarity of the chemical shifts. Note that taking the ratio of $N_Z^{sat}(t)$ and $N_Z^{nonsat}(t)$ at a sufficiently long delay time, a correct NOE value is obtained. The $N_Z^{sat}(t)$ values are used to determine relaxation time, T_1^{sat}, using a single exponential recovery function. The solid lines are the fit recovery curve

NOE experiments with a sufficient signal-to-noise ratio. For residues 8 and 9 (Fig. 2a, b), the ^{15}N magnetization intensity recorded in the absence of ^1H saturation, $N_Z^{nonsat}(t)$, is larger than that recorded in the presence of ^1H saturation, $N_Z^{sat}(t)$ at any time duration. In contrast, for residues 5 and 6, the magnetization intensity in the presence of ^1H saturation becomes larger than the non-saturation recovery intensity for delays less than 4 s (Fig. 2c, d). For the latter case (Fig. 2c, d), if the NOE value is calculated using the intensities recorded using delays in the range of 1–3 s, the measured NOE values, NOE_m, becomes larger than 1.0.

According to Eq. (2), $N_Z^{sat}(t)$ relaxes as $(1 - \exp(-t/T_{1N}))$. On the other hand, the relaxation of $N_Z^{nonsat}(t)$ is more complex, as described by Eq. (1). The difference in the decay between $N_Z^{nonsat}(t)$ and $N_Z^{sat}(t)$ is in the second terms of Eqs. (1) and (2), and results in the NOE_m ($N_Z^{sat}(t)/N_Z^{nonsat}(t)$) expressed by Eq. (4). When $T_{1H} > T_{1N}$ and $t > T_{1N}$, f defined by Eq. (5) is always less than 1. When $t > 1$ s, this is true in a small protein that does not experience extensive spin-diffusion. In the condition of $0 < f < 1$, the NOE_m must be less than 1.0 for all values of t because the subtraction of denominator from numerator, NOE – (1–f(1–NOE)) = (NOE–1)(1–f), becomes negative. Thus, Eqs. (4) and (5) do not properly correct the measured NOE values when $NOE_m > 1.0$. Overall, the observed magnetization recovery in Fig. 2c, d can not be explained by the Solomon equation.

Experimental investigation of the violation of the Solomon equations

These violations from the Solomon equations are not limited to a small number of residues. As shown in Fig. 3a, many residues have $NOE_m > 1.0$ when the recovery time is set to 3 s in both experiments in the presence and absence of ^1H saturation, i.e., in the case of $NOE_m(3,3)$. When the decay becomes sufficiently long, ca. 6 s in the absence of ^1H saturation and 4 s in the presence of ^1H saturation, $NOE_m(4,6)$ values are mostly less than 0.9, values that are consistent with the theoretically estimated NOE values. The sites that have $NOE_m(3,3)$ larger than 1.0 generally exhibit longer ^1H T_1 values (>3 s) (Fig. 3b). Holak's group has also previously pointed out that mobile regions exhibit $NOE_m > 1.0$ when the pulse repetition delay time is small, although an explanation was not provided for this observation (Renner et al. 2002).

To understand why NOE_m values >1.0 are observed (or $N_Z^{nonsat}(t) < N_Z^{sat}(t)$), we investigated which magne-

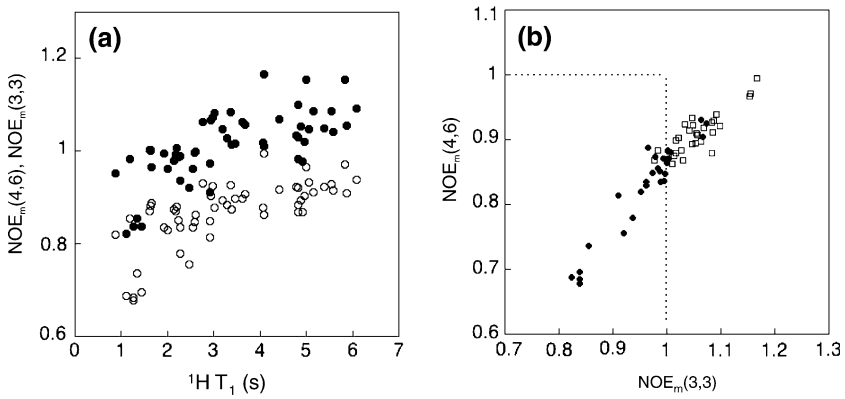

Fig. 3 (**a**) Plots of measured ^{15}N–{^{1}H} NOE values against ^{1}H longitudinal relaxation time (T_1). (**b**) Plot of measured ^{15}N–{^{1}H} NOE values versus ^{15}N–{^{1}H} NOE values determined using different recovery times. In (**a**), plots are shown for the ^{15}N–{^{1}H} NOE values determined using the 3 s recovery magnetization recovery in both presence and absence of ^{1}H saturation (*filled circle*, NOE$_m$(3,3)), and also shown for the ^{15}N–{^{1}H} NOE values determined using the 4 s recovery magnetization recovery in the presence of ^{1}H saturation and 6 s recovery in the absence of ^{1}H saturation (*open circle*, NOE$_m$(4,6)). In (**b**), plots are shown for NOE$_m$(4,6) versus NOE$_m$(3,3). In (**b**), open squares indicate the amide sites that exhibit ^{1}H T_1 values longer than 3 s

tization recovery, $N_Z^{nonsat}(t)$ or $N_Z^{sat}(t)$, differs from the predictions of the Solomon equation. Equation (2) predicts that $N_Z^{sat}(t)$ relaxes by a single exponential function characterized by ^{15}N T_1. Therefore, we determined the relaxation time obtained from the magnetization recovery of $N_Z^{sat}(t)$, T_1^{sat}, and compared it with the ^{15}N T_1 determined by the inversion recovery method. Figure 4 shows a correlation between the ^{15}N T_1^{sat} and ^{15}N T_1. In spite of a small systematic difference of 0.03 s, the ^{15}N T_1^{sat} values are highly correlated with the ^{15}N T_1 values. Possible mechanisms that cause the systematic difference are (1) insufficient suppression of the DD-CSA effect, or (2) lack of full recovery intensity, $N^{sat}(\infty)$. First, we think that the lack of full recovery intensity may introduce larger errors in longer T_1^{sat} but is not expected to cause a systematic increase in T_1^{sat} values. Second, regarding the suppression of the DD-CSA effect, we measured the efficiency of ^{1}H saturation (data not shown) and found a similar result to that of Holak's group (Renner et al. 2002) in which ^{1}H magnetization is almost instantaneously reduced by over 90%. Since the apparent relaxation time changes ca. 60% (1.89 and 1.18 s in Fig. 6) with and without the cross-correlation suppression, the 10% remained proton signals perturbed by 120° pulses may cause the slight increase of the relaxation time. Nevertheless, 0.03 s difference (less than 5% of ^{15}N T_1^{-1}) in ^{15}N T_1^{sat} from ^{15}N T_1determined by inversion recovery is too small to make the recovery of $N^{sat}(t)$ magnetization faster than $N_Z^{nonsat}(t)$ magnetization. Overall, ^{15}N magnetization recovery in the presence of ^{1}H saturation, $N_Z^{sat}(t)$, is consistent with the prediction of the Solomon equations.

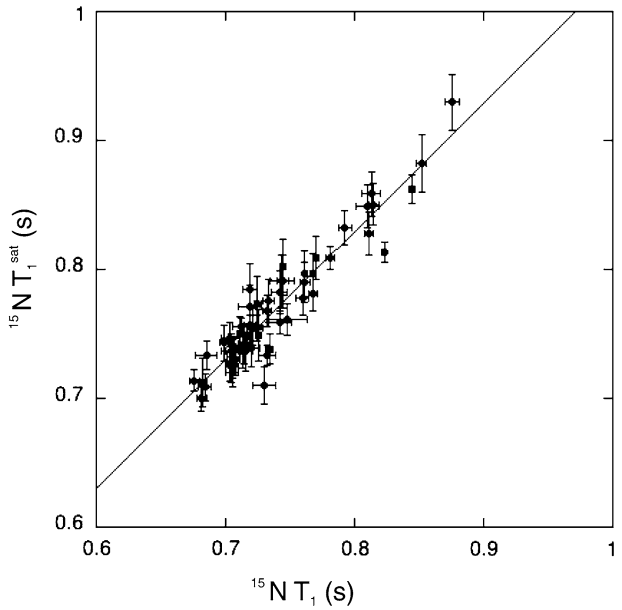

Fig. 4 Plot of ^{15}N relaxation rate determined in the presence of ^{1}H saturation, T_1^{sat}, versus ^{15}N T_1 values determined by conventional inversion recovery experiment

To understand whether the time dependence of $N_Z^{nonsat}(t)$ magnetization differs from the prediction of the Solomon equations, we recorded relaxation of the N_ZH_Z two-spin order because the DD-CSA cross-correlation is expected to be significant if the proton spin-flip time, T_{sf}, is similar to or longer than the ^{15}N relaxation time. As shown in Fig. 5, the T_{sf} values are 0.4–2.0 s, which are compatible to those of ^{15}N T_1, which indicates that the DD-CSA cross-correlation may have a significant contribution in $N_Z^{nonsat}(t)$ recovery. Since the effect of the cross-correlation was

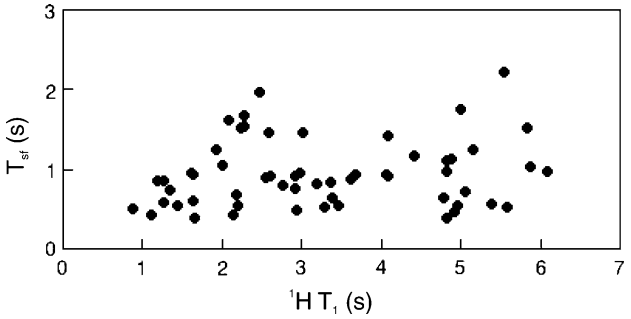

Fig. 5 Plot of proton spin-flip time, T_{sf}, versus proton T_1. The spin-flip time was calculated based on Eq. (6) using the $2N_ZH_Z$ relaxation time and ^{15}N T_1

not taken into account in the two-spin Solomon equations described above (Eqs. 1 and 2), quantitative evaluation of the effects of CSA/dipolar cross-correlation on $N_Z^{nonsat}(t)$ will be required.

Although DD-CSA cross-correlation effects on ^{15}N T_1 and T_2 have been studied and pulse sequences to suppress the effect have been published, the DD-CSA effect on ^{15}N T_1 was observed to be relatively small. This is partly because the effect was partially suppressed by relatively rapid proton spin flips in protonated proteins and partly because these earlier studies used low magnetic field strengths (Boyd et al. 1990; Kay et al. 1989).

Interestingly, the T_{sf} values did not have a clear correlation with the ^{1}H T_1 values (Fig. 5). This lack of correlation is presumably because T_{sf} primarily decreases with increase in the effective correlation time and the number of dipolar interactions, whereas ^{1}H relaxation time, T_1, decreases with an increase in the number of dipolar interactions but increases with an increase in the effective correlation time.

Simulation of ^{15}N magnetization relaxation

To understand the effect of DD-CSA cross-correlation on the recovery of magnetization, we simulated relaxation of the longitudinal magnetizations including the DD-CSA cross-correlation mechanism in the relaxation matrix. First, we tested a simple relaxation in which initial magnetization of $[N_Z^0, H_Z^0, N_ZH_Z^0] = [1, 0, 0]$ relaxes to $[0, 0, 0]$ with an effective correlation time of 6.5 ns and ^{1}H T_{sp}^{-1} of 1.5 s^{-1} (Fig.6, using simulation (1) in Methods). This effective correlation time includes the amplitude reduction of the spectral density function by internal motion, and is larger than the actual rotational correlation time estimated for ubiquitin at 17°C. The T_{sf} value used in the simulation is within the range observed in the experimental result in Fig. 5. As shown in Fig. 6, two components of ^{15}N longitudinal magnetization (see Methods), $N^{(1)}$ and $N^{(2)}$, decay at different rate due to the DD-CSA cross-correlation effect. However, the difference in the intensities between the two components is small at a 500 MHz ^{1}H-NMR frequency. For example, at 3 s duration of a decay time, the difference of the intensity between $N^{(1)}$ and $N^{(2)}$ is 1.7% of the initial $N^{(1)}$ (= 0.5 N_Z^0) whereas the difference of the intensity is 12.7% at 3 s duration assuming a 800 MHz instrument (Fig. 6). This increase of the discrepancy between $N^{(1)}$ and $N^{(2)}$ at higher magnetic field strength is reasonable because chemical shift anisotropy increases as the magnetic field strength increases, and makes the cross-correlation effects increase (Boyd et al. 1990; Kay et al. 1989). The apparent T_1 value determined for the magnetization recovery of the summation of $N^{(1)}$ and $N^{(2)}$ magnetizations (using 11 points of time duration from 0 to 3 s which corresponds to the range used to detect magnetization recovery in the NOE experiments) became 1.89 ± 0.076 s, which is considerably longer than the T_1 value (1.18 s) that does not include the cross-correlation effect. The 1.6 times longer T_1 explains why $N_Z^{nonsat}(t)$ magnetization relaxes slower than estimated from the Solomon equation.

Next, we simulate the magnetization recovery in the absence of ^{1}H saturation and compared the recovery in the presence of ^{1}H saturation (simulation (2) in

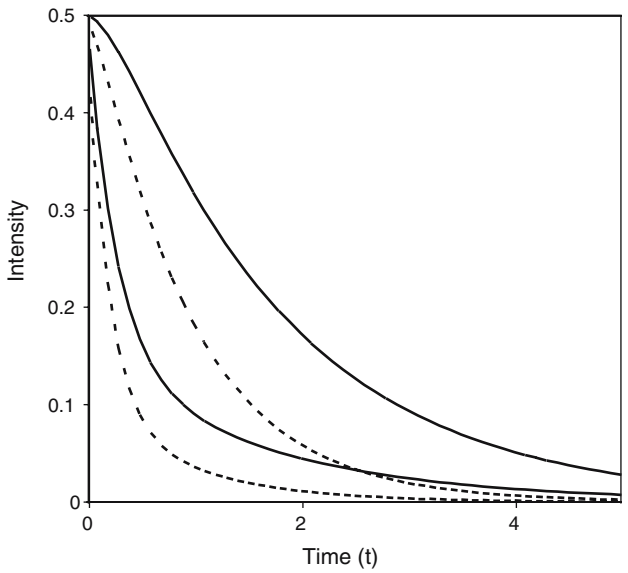

Fig. 6 Simulated decay of intensity of $N^{(1)}$ and $N^{(2)}$ components at 500 MHz (*broken lines*) and 800 MHz (*solid lines*). Proton spin flip (T_{sf}^{-1} = 1.5 s^{-1}) and external proton relaxation (0.5 s^{-1}) in addition to N–H interaction were taken into account for the calculation. The simulation assumes an effective rotational correlation time of 6.5 ns

Methods). We simulated the later curve as an exponential recovery with T_1 = 0.7 s towards the saturation intensity of 0.85, which is the maximum NOE value at an effective correlation time of 6.5 ns. The simulation in the absence of ^{1}H saturation was achieved by assuming T_{sf}^{-1} = 1,000 s^{-1} in which the spin-flip is very quick relative to the average relaxation (or recovery) of the two components (Fig. 7a). The simulation in the absence of ^{1}H saturation was performed including the DD-CSA cross-correlation effect in which T_{sf}^{-1} was assumed to be 1.5 s^{-1} (Fig. 7b). The $N_Z(t)$ magnetization plotted in Fig. 7 is the sum of $N^{(1)}(t)$ and $N^{(2)}(t)$. When the DD-CSA effect is suppressed by the fast spin-flip, the magnetization recovery calculated in the absence of ^{1}H saturation is always larger than that in the presence of saturation (Fig. 7a). However, when cross-correlation is significant, the magnetization recovery in the absence of ^{1}H saturation becomes so slow that the magnetization in the absence of ^{1}H saturation becomes smaller than that in the presence of ^{1}H saturation during the recovery duration up to 3 s (Fig. 7b). Figure 7a adequately describes the situations depicted in Fig. 1a and b whereas the Fig. 7b describes that in Fig. 1c and d.

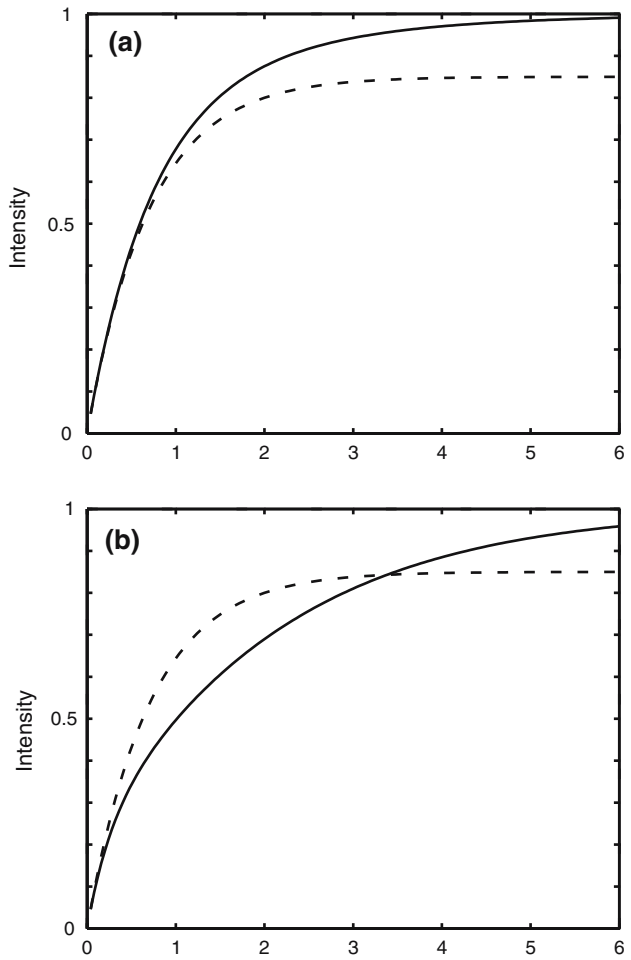

Fig. 7 Simulated magnetization recovery (**a**) when proton spin flip is fast (T_{sf}^{-1} = 1,000 s^{-1}) and (**b**) when proton spin flip is slow (T_{sf}^{-1} = 1.5 s^{-1}) in the absence of ^{1}H saturation (*solid lines*). Broken lines are magnetization recovery curves in the presence of ^{1}H saturation, which is calculated as a single exponential recovery characterized by ^{15}N T_1 which was assumed to be 0.7 s. The simulation assumes an effective rotational correlation time of 6.5 ns and the 800 MHz proton operating frequency

Although the magnetization recovery in the absence of ^{1}H saturation is not rigorously a single exponential function because of the ^{1}H–^{15}N cross-relaxation effect (Eq. 1), the above differences in magnetization recoveries are more adequately characterized by fitting as a single exponential curve. The approximate relaxation time of the magnetization recovery calculated from the solid curve of Fig. 7a (in the absence of ^{1}H saturation, with suppression of the cross-correlation) becomes 0.9 s. This value is slightly larger than the ^{15}N T_1 (0.7 s) of magnetization recovery in the presence of ^{1}H saturation, with the difference due to the ^{1}H/^{15}N cross-relaxation. On the other hand, the approximate relaxation time of magnetization decay calculated from the solid curve of Fig. 7b (in the absence of ^{1}H saturation, without suppression of the cross-correlation) becomes 1.53 s, which is almost twice longer than the ^{15}N T_1.

Correlation time dependence of NOE $N^{(1)}$ and $N^{(2)}$

As described in the above section, the magnetization recovery time in the absence of ^{1}H saturation for the ^{15}N-{^{1}H} NOE experiment becomes significantly longer than the recovery time estimated based on the Solomon equations. This phenomenon becomes evident at high magnetic field strength as shown in Fig. 6. We will therefore calculate the intensities of the $N^{(1)}$ and $N^{(2)}$ as a function of an effective correlation time. To simulate $N^{(1)}$ and $N^{(2)}$ intensities at different effective correlation times, the amount of external ^{1}H–^{1}H dipolar interaction and proton spin flip rate are given by a function of the effective correlation time. In this calculation, ^{1}H–^{1}H dipolar interactions with external protons are tentatively simulated by an effective interaction with a single proton with an internuclear distance, r_H, of 2.7 Å and 1.9 Å for a deuterated and a protonated protein, respectively.

A previous study by Bax and colleagues indicates that $2I_ZS_Z$ relaxation time of calcium loaded calmodulin is in the range of 50–130 ms (T_{sf}^{-1} in the range of 6–19 s^{-1}) with an apparent rotational correlation time of 6–7 ns (Kay et al. 1992). Figure 5 shows T_{sf}^{-1} of the deuterated ubiquitin becomes ca. 1.5 s^{-1}. In our tentative model, T_{sf}^{-1} for protonated (r_H = 1.9 Å) and

deuterated (r_H = 2.7 Å) proteins at 7 ns correlation time are calculated to be 8 and 1 s^{-1}, respectively. Although our model may underestimate the T_{sf}^{-1} of protonated proteins at larger correlation times, this model will elucidate the qualitative difference of T_{sf}^{-1} effects on $N^{(1)}$ and $N^{(2)}$ between a protonated protein and a deuterated protein.

At 800 MHz for a deuterated protein (r_H =2.7 Å) (Fig. 8a, solid lines) there is a significant difference in the signal intensities of $N^{(1)}$ and $N^{(2)}$ components at 3 s recovery time at effective correlation time less than 20 ns. The difference in the $N^{(1)}$ and $N^{(2)}$ intensities is diminished at an extremely high correlation time (>30 ns) due to efficient spin diffusion, even though the proton density is low. On the other hand at 500 MHz (Fig. 8a, broken lines), both of the $N^{(1)}$ and $N^{(2)}$ components are more relaxed after a 3 s duration when the correlation time is in the range of 2–10 ns, indicating that $\{^1H\}$–^{15}N NOE data can be measured with a relatively small error, using 3 s duration even for a deuterated protein at 500 MHz. However, Fig. 8a also predicts that even at 500 MHz, the $N^{(1)}$ and $N^{(2)}$ components relax significantly differently due to the CSA-DD cross-correlation when the effective correlation time is less than 2 ns.

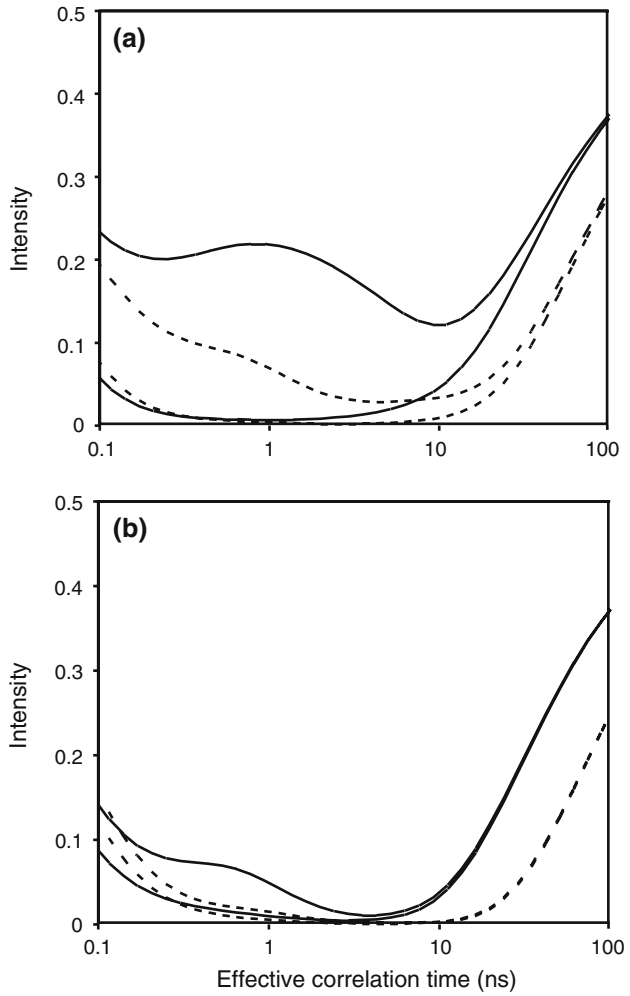

Fig. 8 Simulated intensity of $N^{(1)}$ and $N^{(2)}$ components at 500 MHz (*broken lines*) and 800 MHz (*solid lines*) at 3 s delay versus the effective rotational correlation time. Simulations were performed using a model which includes a single ^1H–^1H dipolar interaction with a distance of (**a**) 2.7 Å and (**b**) 1.9 Å assuming deuterated and protonated proteins, respectively (see Methods)

Assuming a protonated protein (r_H = 1.9 Å), the $N^{(1)}$ and $N^{(2)}$ components relax almost simultaneously at the correlation times more than 2 ns, even at 800 MHz (Fig. 8b, solid line). This prediction indicates that although the magnetization recovery of a molecule at an effective correlation time of >10 ns is not completed at 3 s, the measured NOE values can be corrected using Eqs. (4) and (5). This equality of $N^{(1)}$ and $N^{(2)}$ at 800 MHz is similar to that of 500 MHz (Fig. 8b, broken line). However, even in protonated proteins, at correlation times less than 2 ns at 800 MHz (Fig. 8b), the spin flip rate becomes insignificant, and the $N^{(1)}$ and $N^{(2)}$ components relax significantly differently due to the CSA-DD cross-correlation. Therefore, the correction equation may not be applicable for a small protein or mobile regions even when the protein is protonated. This prediction qualitatively agrees to the experimental results published by Holak (Renner et al. 2002).

Design of NOE experiment

These simulations indicate that DD-CSA effect is evident for the system that has slow proton spin-flip rate, i.e., deuterated protein or small protein. A simple solution is to record the NOE experiments at lower magnetic field strength, such as 500 MHz or 600 MHz. Nevertheless, it is technically possible to suppress the DD-CSA cross-correlation effects using two ^{15}N 180° pulses during the magnetization recovery (Fig. 1b). Note that in this sequence, the sign of the cross-relaxation does not flip because the sign of the ^1H magnetization does not change. As shown in Fig. 9, the NOE(^{15}N_flip) values measured by using this sequence (Fig. 1b) are mostly less than 1.0, even at 2 s delay. A drawback is that the insertion of the ^{15}N pulses during the magnetization recovery period complicates the ^{15}N magnetization recovery itself, and terribly reduces signal-to-noise ratio of the experiment due to insufficient the recovery of N_Z magnetization due to the 180° pulses. As compared with the correlation between NOE_m(3,3) and NOE_m(4,6) (Fig. 3b), the correlation between NOE(^{15}N_flip) and NOE_m(4,6) (Fig. 9) is not

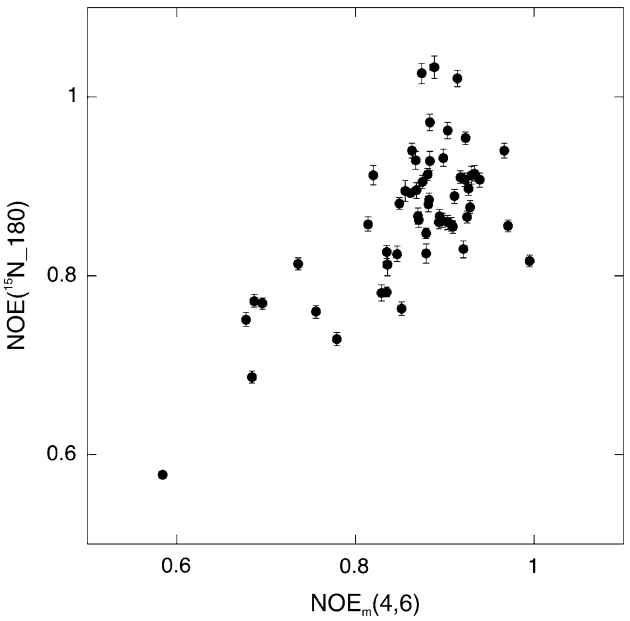

Fig. 9 Plots of ^{15}N–{^{1}H} NOE values measured using the two ^{15}N pulses during the recovery delay (Fig. 1b scheme) versus NOE(4,6) shown in Fig. 3

significant presumably because of the complexity of the recovery profile. Therefore, this experiment is only proposed to demonstrate the cross-correlation effect on the NOE experiments, but is not recommended for practical applications.

Practically, for the systems with slow proton spin-flip rates, since the correction equations (Eqs. 4–5) cannot be used, it is necessary to wait a sufficient delay time when the NOE experiments are performed in a high field magnets. However, we emphasize again that we do not need to wait for the same delay time for both experiments performed in the presence and absence of proton saturation (Renner et al. 2002). Since the ^{15}N magnetization recovery in the presence of saturation is basically characterized by the ^{15}N T_1, the experiment in the presence of ^{1}H saturation can be set shorter than that in the absence of the ^{1}H saturation: for example, ca. 3 s and 6 s respectively. As described previously, the delay time in the absence of ^{1}H saturation has to be longer to obtain accurate NOE value for mobile region (Renner et al. 2002).

In summary, we have explained why $N_Z^{sat}(t)$ intensity becomes larger than the $N_Z^{nonsat}(t)$ intensity during the magnetization recovery in the ^{15}N–{^{1}H} NOE experiment, quantitatively by taking into account the DD-CSA cross-correlation effect, using experiments and simulations. We also clarified under what conditions the DD-CSA significantly affects magnetization recovery for NOE experiments.

Acknowledgements We thank Dennis Torchia in NIDCR, NIH, for providing us with the original MATLAB program to calculate magnetization recovery and for critical reading of the manuscript. We also thank Kwaku Dayie in Cleveland Clinic and Joseph Walsh in University of Pittsburgh for critical reading and correction of the manuscript.

References

Boyd J, Hommel U, Campbell ID (1990) Influence of cross-correlation between dipolar and anisotropic chemical shift relaxation mechanims upon longitudinal relaxation rates of 15N in macromolecules. Chem Phys Lett 175:477–482

Bruschweiler R (2003) New approaches to the dynamic interpretation and prediction of NMR relaxation data from proteins. Curr Opin Struct Biol 13:175–183

Cavanagh J, Fairbrother WJ, Palmer AG, Skelton NJ (1996) Protein NMR spectroscopy. Academic Press, San Diego

Dayie KT, Wagner G, Lefevre JF (1996) Theory and practice of nuclear spin relaxation in proteins. Annu Rev Phys Chem 47:243–282

Delaglio F, Grzesiek S, Vuister GW, Zhu G, Pfeifer J, Bax A (1995) NMRpipe – a Multidimensional Spectral Processing System Based on Unix Pipes. J Biomol NMR 6:277–293

Freedberg DI, Ishima R, Jacob J, Wang YX, Kustanovich I, Louis JM, Torchia DA (2002) Rapid structural fluctuations of the free HIV protease flaps in solution. Protein Sci 11:221–232

Freeman R, Hill HDW (1971) Fourier Transform Study of NMR Spin-Lattic Relaxation by ''Progressive Saturation''. J Chem Phys 54:3367–3377

Fushman D, Cowburn D (2001) Nuclear magnetic resonance relaxation in determination of residue-specific N-15 chemical shift tensors in proteins in solution: Protein dynamics, structure, and applications of transverse relaxation optimized spectroscopy. Methods Enzymol 339:109–126

Garrett DS, Gronenborn AM, Clore GM (1995) Automated and Interactive Tools for Assigning 3d and 4d Nmr-Spectra of Proteins – Capp, Stapp and Pipp. J Cell Biochem Supple 21B:71

Goldman M (1984) Interference effects in the relaxation of a pair of unlike spin-1/2 nuclei. J Magn Reson 60:437–452

Grzesiek S, Bax A (1993) The Importance of Not Saturating H_2O in Protein NMR – Application to sensitivity enhancement and noe measurements. J Am Chem Soc 115:12593–12594

Igumenova TI, Frederick KK, Wand AJ (2006) Characterization of the fast dynamics of protein amino acid side chains using NMR relaxation in solution. Chem Rev 106:1672–1699

Ishima R, Torchia DA (2000) Protein dynamics from NMR. Nat Struct Biol 7:740–743

Jarymowycz VA, Stone MJ (2006) Fast time scale dynamics of protein backbones: NMR relaxation methods, applications, and functional consequences. Chem Rev 106:1624–1671

Kay LE (2005) NMR studies of protein structure and dynamics. J Magn Reson 173:193–207

Kay LE, Torchia DA, Bax A (1989) Backbone dynamics of proteins as studied by nitrogen-15 inverse detected heteronuclear NMR spectroscopy: application to staphylococcal nuclease. Biochemistry 28:8972–8979

Kay LE, Nicholson LK, Delaglio F, Bax A, Torchia DA (1992) Pulse sequences for removal of the effects of cross correlation between dipolar and chemical-shift anisotropy relaxation mechanisms on the measurement of heteronuclear T1 and T2 values in proteins. J Magn Reson 97:359–375

Li YC, Montelione GT (1994) Overcoming solvent saturation-transfer artifacts in protein NMR at neutral pH – Application of pulsed-field gradients in measurements of H-1 N-15 Overhauser effects. J Magn Reson Ser B 105:45–51

Muhandiram DR, Yamazaki T, Sykes BD, Kay LE (1995) Measurement of H-2 T-1 and T-1p Relaxation-Times in Uniformly C-13-Labeled and Fractionally H-2-Labeled Proteins in Solution. J Am Chem Soc 117:11536–11544

Palmer AG 3rd (1997) Probing molecular motion by NMR. Curr Opin Struct Biol 7:732–737

Palmer AG 3rd (2001) NMR probes of molecular dynamics: overview and comparison with other. Annu Rev Biophys Biomol Struct 30:129–155

Palmer AG, Skelton NJ, Chazin WJ, Wright PE, Rance M (1992) Suppression of the effects of cross-correlation between dipolar and anisotropic chemical-shift relaxation mechanisms in the measurement of spin spin relaxation rates. Mol Phys 75:699–711

Redfield C (2004) Using nuclear magnetic resonance spectroscopy to study molten globule states of proteins. Methods Mol Biol 34:121–132

Renner C, Schleicher M, Moroder L, Holak TA (2002) Practical aspects of the 2D N-15-{H-1}-NOE experiment. J Biomol NMR 23:23–33

Skelton NJ, Palmer AG, Akke M, Kordel J, Rance M, Chazin WJ (1993) Practical aspects of 2-dimensional proton-detected N-15 spin relaxation measurements. J Magn Reson Ser B 102:253–264

Sklenar V, Torchia DA, Bax A (1987) Measurement of carbon-13 longitudinal relaxation using 1H detection. J Magn Reson 73:375–379

Solomon I (1955) Relaxation processes in a system of two spins. Phys Rev 99:559–565

Werbelow LG, Grant DM (1977) Intramolecular dipolar relaxation in multispin systems, p. 189–299. In: Waugh JS (ed) Advances in magnetic resonance, vol 9. Academic Press, New York, pp 189–299